

Helena: Real-time Contact-free Monitoring of Sleep Activities and Events around the Bed

Jose Clemente^{1†}, Maria Valero^{1,3†}, Fangyu Li¹, Chengliang Wang² and WenZhan Song¹

¹Center for Cyber-Physical Systems, University of Georgia, Athens, USA

²College of Computer Science, Chongqing University, Chongqing, China.

³Intelligent Dots LLC, Alpharetta, USA

Abstract—In this paper, we introduce a novel real-time and contact-free sensor system, Helena, that can be mounted on a bed frame to continuously monitor sleep activities (entry/exit of bed, movement, and posture changes), vital signs (heart rate and respiration rate), and falls from bed in a real-time and pervasive computing manner. The smart sensor senses bed vibrations generated by body movements to characterize sleep activities and vital signs based on advanced signal processing and machine learning methods. The device can provide information about sleep patterns, generate real-time results, and support continuous sleep assessment and health tracking. The novel method for detecting falls from bed has not been attempted before and represents a life-changing for high-risk communities, such as seniors. Comprehensive tests and validations were conducted to evaluate system performances using FDA approved and wearable devices. Our system has an accuracy of 99.5% detecting on-bed (entries), 99.73% detecting off-bed (exits), 97.92% detecting movements on the bed, 92.08% detecting posture changes, and 97% detecting falls from bed. The system estimation of heart rate (HR) ranged ± 2.41 beats-per-minute compared to Apple Watch Series 4, while the respiration rate (RR) ranged ± 0.89 respiration-per-minute compared to an FDA oximeter and a metronome.

Index Terms—Sleep monitoring, vibration, fall detection, advanced signal processing, machine learning.

I. INTRODUCTION

Currently, 654 million people are 65 years and older worldwide [1], and around 47.8 million live in the United States [2]. Within those people, nearly 26% live alone at home and 18% in senior healthcare facilities or similar according to U.S Census Bureau [2]. In this population, there is a lack of contact-free and privacy-preserving solutions for monitoring sleep activities. Most of the monitoring solutions in the market are conceived to measure just vital signs (heart rate) with a wearable apparatus/gadget, and those do not detect other important activities like lack of movement on the bed and falls from bed. Other devices require person actions, like pressing a button when a fall happens, but those cannot be activated if the person loses the conscience. On the other hand, the use of cameras to monitor sleep generally raises privacy concerns.

This paper introduces a novel real-time and contact-free sensor system that can be mounted on the bed frame to continuously monitor sleep activities (entry/exit of bed, movement, and posture changes) and vital signs (heart rate, respiration rate),

and falls from bed. The technology includes a small yet smart vibration sensor that can be easily installed and a user-friendly graphic interface that can be paired with smart mobile devices to monitor results through a software application. Vibration sensors have been widely used in smart home applications [3]–[6]. The smart sensor senses bed vibrations generated by body movements and sleep activities and then infers sleep activities and vital signs based on advanced signal processing and machine learning methods. The system provides information about sleep patterns, generates real-time results, and supports continuous sleep assessment and health tracking.

The main contributions of our work are:

- A real-time contact-free sleep monitoring system based on bed vibration, which allows estimation of heart and respiration rates as well as sleep activities like on/off bed detection, movements, posture changes, and for the first time falls from bed. The system allows sending alerts to smart devices when sudden changes occur, for example, the person has too many or too few movements, a fall down happens, or the person entry/leaves the bed.
- Accurate, light and fast methods for heart and respiration rates, suitable for pervasive devices, that can be executed in real-time on a single-board computer.
- First work to propose a method to detect and alert falls from bed using only vibration signals.
- First work to propose a method to detect movement and postures changes based only on the vibration signal generated by the body on the bed.

II. RELATED WORKS

Sleep monitoring is extremely important, even a lifesaver, for people with undiscovered illness, which causes respiration and heart failures [7], [8]. The respiration status can be monitored by breathing apparatuses [9], while the heart rate is typically measured by wearable devices [7]. However, those devices need body contact and are intrusive. Many people feel not comfortable to wear or forget to wear before sleep. Comparing with FDA approved wearable devices, our system can identify with high accuracy sleep activities and vital signs. Furthermore, to the best of our knowledge, this is the first work that proposes a method to detect falls from bed using only vibration signals. There are multiple contact-based devices for sleep monitoring. For example, wearable devices like *Apple Watch* [10], *Jawbone 3* [11], *Basis Peak* [12], *Fitbit Surge* [13], and a number of other

The research is partially supported by NSF-STTR-1940864 and NSF-1663709.

[†]: Both authors contributed equally to this work.

“smartwatch” devices that have been good in demonstrated their capabilities to measure heart rate; however, they lack deep study of activities and patterns behaviors of the person during night and require user intervention for correct performance. Undermattress devices like *Beddit* [14] and *Nokia Withings Sleep Tracking Pad* [15] measure sleep time, heart and respiration rates, sleep cycles; however, these measurements are based on a whole night average that is shown the next day, which means there is not real-time information. EarlySense device [16] is the most near to real-time sleep monitoring and has been developed to provide continuous monitoring of heart rate, respiration rate, and bed motion for patients in medical/surgical scenarios using a pressure sensor; however, it does not detect posture changes and fall from bed and it is really expensive. Seismometers, including geophones, have been widely used in geophysical and civil engineering applications [17]–[20]. Recently, new applications for smart environments are explored, such as ambient floor vibration for indoor person localization [6], [21], bed vibration for heart beating and breathing rate monitoring [22]–[24], etc, but those applications are not real time. Besides, there have been rare work on sleep posture identification using body vibration patterns during sleep.

III. OVERVIEW

We use a smart sensor composed by a geophone (seismic sensor) [25], [26], a digitizer board and a single-board computer (Raspberry Pi 3B) [27]. It is shown in Fig. 1. The geophone detects the velocity of the movements. The digitizer transforms analog vibration signals to digital that is read by the single-board computer. The single-board computer reads and processes the signal to estimate the vital signs and on bed activities. After multiple tests, we decide that the sensor must be installed in a range no larger than 40 centimeters from the heart location when the person lying down. The estimated results are sent to the Cloud used the single-board computer WiFi. Also, it is in charge of sensing alert messages via email or/and SMS and to communicate with the smart assistant (Google Home or Amazon Echo).



Fig. 1: Helena unit prototype.

Fig. 2 illustrates Helena architecture. The raw data sensed by the geophone is used to determine the bed status (on/off/sitting). If the person is detected on bed, Helena cleans the noise and estimates HR and RR if there are no movements in the last 15 seconds. It is the time window used to calculate the vital signs with high accuracy. The vital signs are estimated every 3 seconds. When a movement is detected, we evaluate three scenarios (posture change, off bed and fall from bed). We

use 5 seconds of data before and after the event to calculate posture change. For fall from the bed, we analyze if after the movement there is an off-bed status. Then, the system performs a machine learning model to detect if the event is a fall from the bed. Otherwise, an off-bed event is set.

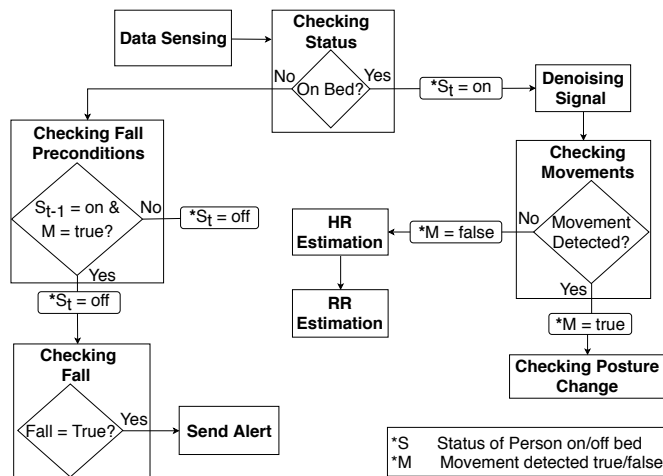


Fig. 2: Helena Architecture.

Additionally, we develop a real-time visualization tool based on InfluxDB [28] and Grafana [29]. The raw data are stored in a local database, and results are sent to the cloud. Grafana is used to create the dashboards for raw data, bed status (on/off/sitting), HR, RR, movement, posture change and fall from bed.

IV. CHALLENGES

There are three main challenges to estimate sleep activities and vital signs using a vibration signal captured by a sensor attached on the bed frame:

- **Ambient noises:** In the vibration-based systems, the main issue is the unpredictable noise generated by natural and human activities. Constant noise, like the one produced by an air-conditioner, washer/dryer, vacuum may affect the data quality and vital signs estimation. It is a challenge to detect and eliminate the noises produced by the different machines while preserving the signal produced by the heartbeat. Because Helena is designed for monitoring single person, additional people or pets in bed may general noise.
- **Event recognition:** Vibration-based systems are highly sensitive and can detect other activities besides the heartbeat. A major challenge is to distinguish and classify the relevant events for estimating sleep activities, vital signs, and fall downs, and discard other non-related events.
- **Heartbeat estimation:** The heartbeat signal received by the sensor varies depending on multiple factors like height and type of mattress, sensor location, types of beds. Because heartbeat recognition is the base for many of our algorithms, recognizing heartbeats in different environments/people/setups is a major challenge of the proposed development.

V. ALGORITHM AND SYSTEM DESIGN

A. Signal Enhancing

Since our goal is to realize daily sleep monitoring, the proposed system should be robust to different environments. Besides the random noise suppression, an adaptive machine vibration elimination is also required in the home environment to handle the noises from home appliances, such as AC (air conditioner), washer/dryer, vacuum and so on. Based on the geophone with a 100 Hz sampling rate, the available frequency range is 0~50 Hz, according to the Nyquist sampling theorem. A spectrum scanning method is first applied to remove the machine noises in the environment. We apply notch filters to suppress the noise components with iso-dominant-frequencies. For HR/RR estimation, because the typical HR is between 40 bpm (beat per minute) and 150 bpm and RR is between 12 rpm (respiration per minute) and 25 rpm, which means the target HR/RR should include 0.2 Hz to 2.5 Hz, only a small frequency range is needed. Thus, we apply a bandpass filter with 0.1 Hz low-cut frequency and 8 Hz high-cut frequency to extract target vibration signals. After the process, the machine noise is removed, and the signal retains the vibration signatures.

B. On/Off-Bed - bed exits and entrances

Knowing if the person is effectively lying down on the bed is crucial for other system estimation modules. We propose a Multiple Feature Fusion(MFF) method, that consists of different metrics to estimate if the person has entered or exited the bed. We use a fusion of Spectral Entropy (SE), Kurtosis and Teager Energy Operator (TEO) to estimate the real energy when the person is on the bed. The SE treats the signal's normalized power distribution in the frequency domain as a probability distribution and calculates the Shannon entropy of it. The Shannon entropy in this context is the spectral entropy of the signal. For a signal $x(n)$, the power spectrum is $S(m) = |X(m)|^2$, where $X(m)$ is the discrete Fourier transform of $x(n)$. The probability distribution $P(m)$ is then $P(m) = \frac{S(m)}{\sum_{i=1}^N S(i)}$. Then, the spectral entropy is estimated as $SE = - \sum_{m=1}^N P(m) \log_2 P(m)$.

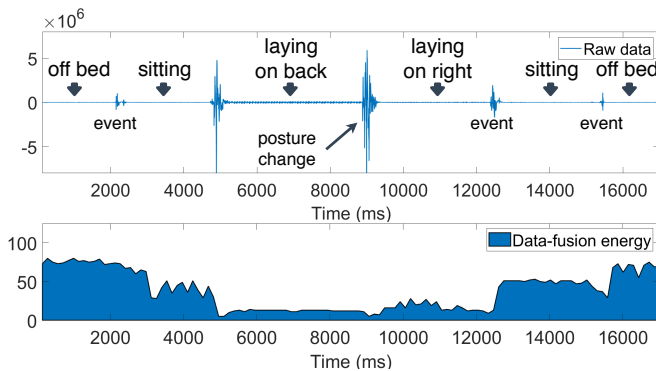


Fig. 3: Data-fusion based entry/exit bed detection.

Kurtosis is the fourth standardized moment, defined as: $Kurt[X] = E \left[\left(\frac{X-\mu}{\sigma} \right)^4 \right] = \frac{\mu_4}{\sigma^4} = \frac{E[(X-\mu)^4]}{(E[(X-\mu)^2])^2}$, where μ is the fourth central moment and σ is the standard deviation. Finally, The TEO can be driven from a second-order differential equation [30]. The total energy of oscillation (i.e., the sum of kinetic and potential energies) can be obtained from the following equation $TEO = \frac{1}{2}kx^2 + \frac{1}{2}m\dot{x}^2$, where m is the mass of the oscillating body and k is the spring constant. Results can be seen in Fig. 3. It is possible to see the decreasing of the total fused energy when the person is on the bed.

C. Movements and Posture Change

To detect movements, we first use the MFF method to determine if the person has entered the bed. After that, we observe that the body movement generates a strong signal (10^7 amplitude) while the respiration and heartbeat show an amplitude about 10^5 . Thus, based on the dramatic energy change, we can recognize the body movement using a local thresholding method:

$$Tr_m = \begin{cases} 1 & \text{if } s(t) \geq \lambda \max(s(z)), z \in (t - \tau, t) \\ 0 & \text{otherwise} \end{cases}, \quad (1)$$

where, $s(t)$ is the signal in time t , λ is a threshold coefficient and τ is the time lag.

Based on the on bed movement detection results, we develop a posture change detection method because not all body movements mean sleep posture changes. For posture change detection, we analyze 5 seconds signal before and after the movement to compare the similarity between them. We calculate the similarity average of four metrics -the Spectral Entropy, Kurtosis, TEO and Power Spectral Density (PSD)- characterized by $sim = \sum_{i=0}^4 (1 - abs(A_i - B_i) / ((A_i + B_i) / 2))$ where, A_i is the metric i value for the signal after the movement, and B_i corresponds the metric i value for the signal before the movement. After several tests, a threshold of $sim < 0.85$ is established to identify if there is a posture change. Fig. 4 shows the signals of different postures for one person.

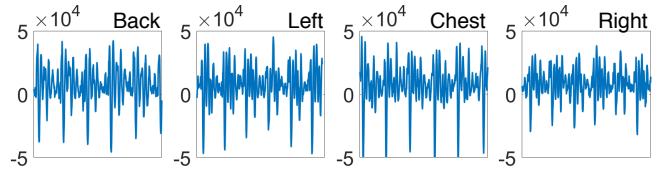


Fig. 4: Five seconds signal from four different postures.

D. HR/RR Estimation

Estimating hearth rate (HR), measured in BPM_h directly from the data spectrum [24] is not accurate because the heartbeat waveform is not strictly periodical in reality as it can be seen in Fig. 5.

The local maxima search method may fail (i.e., generate unreasonable results) when there are noises and other interference. To improve HR estimation stability, we develop an envelope based HR estimation method. The envelope is a curve

such that at each point it touches tangentially the signal. Fig. 5 shows an example of the envelope obtained to estimate in HR. The parametric equations of the envelope are given implicitly as $U(x, u, C) = 0$ and $U'_C(x, u, C) = 0$. Once the envelope is obtained, the peaks can be used to estimate the HR. To solve instabilities, a novel empirical truncated statistics analysis method is proposed to estimate HR. When local maxima of envelope are obtained, there are falsely picked peaks and some missing peaks. Those falsely picked peaks result in smaller period estimation, whereas the missed peaks lead to larger estimation results. Here, X is the interval between two sequential picked peaks. The heartbeat period within $(t - \frac{I_h}{2}, t + \frac{I_h}{2})$ is estimated as a truncated average:

$$E(X|F^{-1}(a) < X \leq F^{-1}(b)) = \frac{\int_a^b xg(x)dx}{F(b) - F(a)}, \quad (2)$$

where, $g(x) = f(x)$ for $F^{-1}(a) < x \leq F^{-1}(b)$;

$g(x) = 0$, everywhere else;

$F^{-1}(p) = \inf\{x : F(x) \geq p\}$.

The lower and upper bounds (a and b) are determined based on the local maxima detection performance. In our applications, 0.1 and 0.9 are chosen for a and b , respectively.

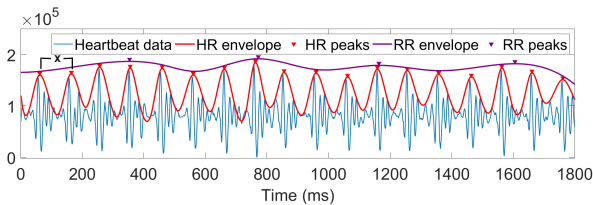


Fig. 5: Heart signal. First and second local maxima estimation from envelope to estimate HR and RR.

Commodity seismometer is insensitive to lower frequency measurements (usually lower than 0.3 Hz) [22], [24], thus the respiratory rate BPM_r can not be directly observed from seismic data. Previously, an amplitude-modulation approach is proposed to use the envelope to estimate carrier frequency [24]. However, the amplitude modulation of the recorded seismic signal is not stable. For that reason, we propose a novel technique to obtain the envelope. We use the HR peaks detected to generate the respiratory modulation signal by extrapolate them. Then we obtain the envelope of the signal and count the peaks to estimate the respiratory rate. Fig. 5 shows the envelope generated by the proposed method.

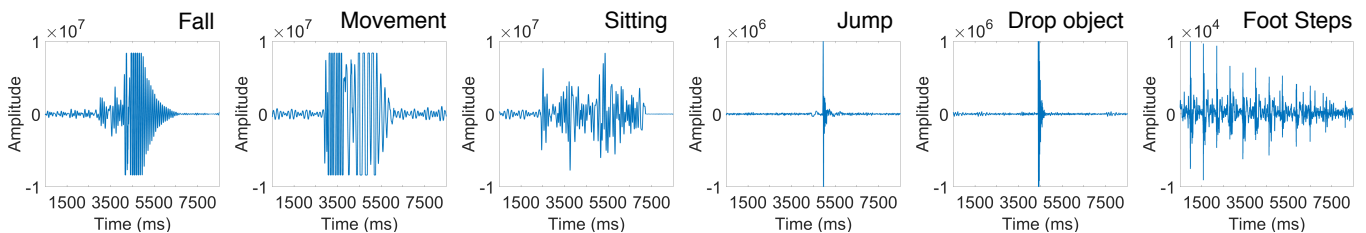


Fig. 6: Bed vibration signals for different events.

E. Fall from Bed

To identify “fall from bed”, we propose to use a machine learning-based approach. Based on a supervised machine learning algorithm, Support Vector Machine (SVM) [31], data are transformed using a kernel to find the optimal boundary between the different classes. SVM and its derivatives have been widely used in the biomedical engineering [6], [32] because it is efficient and easy to implement on embedded devices. Before applying the machine learning method, we identify whether the detected event is a candidate to be a fall from bed. In the stage of “falling from bed”, the person should be laying or sitting on-bed, and then an event needs to be detected. When an off-bed is identified after the event, it becomes a candidate to be a fall from bed. At that moment, the features are extracted and classified by the SVM to identify if the event is a fall from bed or another movement. All events used during training and tests are shown in Fig. 6.

1) **Feature extraction:** We compute features in time and frequency domain. The signal events are normalized to get similar features for each type of events. The normalization is done dividing the event by the energy average of its signal, where the energy is defined as $\mathcal{E} = \sum_{n=0}^N |s(n)|^2$. We use the signal amplitude, event duration, amount of sub-events, and the last 20 peaks information in the time domain. Fig. 7(left) shows the time domain features. In the frequency domain, we select Power Spectral Density (PSD) of the vibration signals, which exposes the power distribution for different frequencies. If s_i represents the signals, then the PSD can be defined as

$$PSD_i = 10 \log_{10} \frac{abs(FFT(s_i))^2}{f_s * n} \quad (3)$$

where f_s is the sampling frequency, n is the number of samples of received signal s_i and $FFT(\cdot)$ is the Fast Fourier Transform operation. Fig. 7(right) shows the PSD feature used as a part of the input.

2) **Selection:** For experimental purposes, we generate 480 simulated falls from bed. To have plenty variety of signals, the simulated falls are performed by 3 people in 4 different bed falling 20 times for each bed-side. To choose the correct classifier that obtains high levels of accuracy and to have the ability to adapt to the limited computing resources of the computer board, we evaluate the accuracy and run-time of three different classifiers using the 480 falls from bed. The tested classifiers are Gaussian Process (GP), K-Nearest Neighbors (KNN) and SVM. The data is split on 80 percent for training

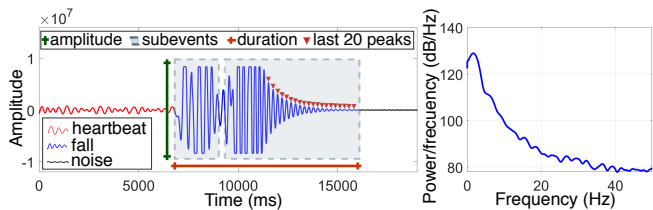


Fig. 7: Time and frequency domain features for fall from bed classification.

and 20 percent for testing. The process was conducted on 4 different Raspberry Pis for each classifier. The results are shown in Table I.

TABLE I: Classifiers performance on “fall from bed” detection. Times are calculated from the average of four Raspberry Pi. Acc (accuracy), Pre (precision), Rec (recall), F1 (F1 score).

Algorithm	Acc	Pre	Rec	F1	Training Time (s)	Classification Time (s)
SVM	90.92	0.69	0.81	0.75	26.146	0.472
KNN	91.33	0.69	0.87	0.77	10.340	12.023
GP	87.83	0.62	0.68	0.65	35.237	2.315

All classifiers have an acceptable level of accuracy. Even though KNN has the highest accuracy and recall, there is no big difference between SVM and GP. On the other hand, all training times are acceptable because they are executed just one time. However, SVM outperforms the classification run-time. The run-time increases 3.2X times when GP classifier is used, and 25.45X times using KNN. Then, we selected SVM as a classification as the classifier model.

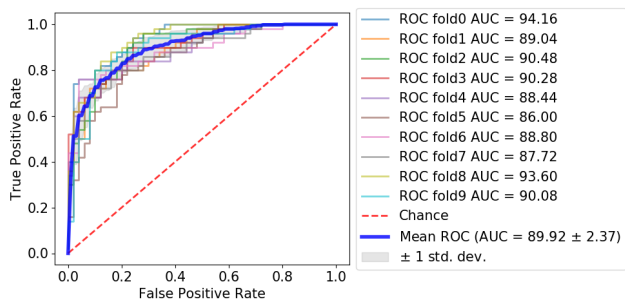


Fig. 8: Receiver Operating Characteristic (ROC) of the cross-validation procedure using 10 folds.

3) **Validation:** The k-fold cross-validation procedure is applied to evaluate the classification model. We use k-fold to estimate how the model is expected to perform when it makes predictions on data not used during the training of the model. The procedure splits the data into k groups, and for each group, it (i) takes one group as a test data set, (ii) takes the remaining groups as a training data set, (iii) fits and evaluates the model, and (iv) retains the evaluation score. We select 10-folds to cross-validate the model. We use AUC (Area Under the Curve) ROC (Receiver Operating Characteristics) to check and visualize the performance of our classification

problem. ROC is a probability curve, and AUC represents the degree or measure of separability. They tell how much model is capable of distinguishing between classes. An excellent model has AUC near to 100, which means it has a good measure of separability. Fig. 8 shows the AUC for all folds. The AUC average is 89.92, which is an acceptable measurement.

VI. EXPERIMENTS AND EVALUATIONS

We performed three types of experiments to validate the bed system. The first one was done in a lab environment to set up parameters, find issues, and validate the system with different people. Then, we carried out a test in different environments outside the lab to test different beds, noise levels, and to validate the HR results comparing with an FDA approved device. Finally, we set up two units in a senior assisted living facility in Loganville, GA to test the system with senior people, crowd environments, and also to get feedback from users, relatives, and nurses.

A. In-lab experiment:

We carried out the first experiment with 10 participants (6 males and 4 females) from our lab and collaborators. It was done in a controlled environment with the same bed and similar background noise. This experiment was done to tune some algorithm parameters and validate the accuracy of on-bed, off-bed, HR, RR, movement, and posture change. For comparison purposes, we used a commercial fingertip pulse oximeter, Zorvo, to obtain continuous readings of the vital signs (HR and RR). The experiment was set up for 18 minutes per participant, and it was distributed as follows (i) 3 minutes on-bed, off-bed and sitting on the bed (ii) 5 minutes for HR, (iii) 2 minutes for RR, (iv) 2 minutes for movements, and (v) 6 minutes for posture change.

1) **On-bed, Off-bed and Sitting experiment:** When the person is on-bed, the system starts the algorithms to calculate the vital signs. We collected 36 bed status from each participant, 12 for each type (on-bed, off-bed, sitting). The participants change the status every 5 seconds according to our directions. In this experiment, the system was set up to detect bed status every 3 seconds. Table II shows the results of the “bed status” test. The method used to calculate the bed status proved to be robust and reliable according to the low error level. The method got a perfect score detecting off-bed because the data-fusion level is high when there is not a periodical signal detected. However, the system detected 9 false on-bed alarms when the participants were seated. Interestingly, after carefully analyzing these specific cases we found that when a person sits in a distance less than 30 centimeters from the sensor, it can detect a faint heartbeat signal that has high auto-correlation levels. We improved the accuracy analyzing the variability between HR peaks, where high variability implies sitting. In some cases, the system can estimate HR if the person is next to the sensor.

2) **Heart rate experiment:** The 5 minutes HR experiment was divided into two blocks. The first is called “resting mode” where the participant lays on the bed for 3 minutes in normal condition. The second, “active mode”, where the participant

TABLE II: Matrix confusion for “bed status” experiment.

	Ground Truth			Evaluation			
	On-bed	Sitting	Off-Bed	Ac	Pr	Re	F1
On-Bed	120	9	0	0.98	0.93	1.00	0.96
Sitting	0	111	0	0.98	1.00	0.93	0.96
Off-Bed	0	0	120	1.00	1.00	1.00	1.00
Avg.				0.98	0.98	0.98	0.97

needs to do exercise for 2 minutes before laying on-bed another 2 minutes to collect high HR and analyze the variation when the person begins to relax. During the experiment, our system was configured to estimate the HR at the same frequency as the oximeter (every 5 seconds). The error was calculated with 36 readings in rest mode and 24 for the active mode per participant. Fig. 9 shows the HR average and the errors obtained in both modes. The estimated average error was 2.35 bpm (beats per minute) for the resting mode and 2.08 bpm for the active mode. The error results were also affected by the error added for the oximeter that is established in 2 bpm in its description. For example, the maximum error obtained during the experiment was 3.43 bpm, but after calculating it manually using the raw data, the real error was 1.26 bpm.

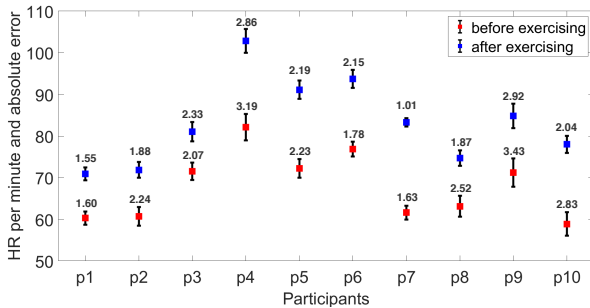


Fig. 9: HR average and mean absolute error from in-lab experiment.

Fig. 10a shows the estimated HRs from the two devices on resting mode. Here, an error from the oximeter can be appreciated at the time 7:35:00 where there is a drop of 10 bpm, and it is recovered after two readings. Fig. 10b shows the HR behavior during the recovery period of the participant after exercising. Both results show a drop of 20 bpm in the first minute, which is considered normal.

3) **Respiration rate experiment:** We used a metronome to validate our respiration rate estimation. The metronome is a generally accepted approach to collect ground truth breathing data in the research community [33], [34]. Even though people are forced to breathe artificially using the metronome, we could estimate the accuracy of our method. The metronome was set to sound every three seconds to get a RR of 20 rpm. Forty readings were collected per participant during the two minutes test. Fig. 11 shows the results obtained for each person and the metronome baseline. The average error was 0.52 rpm validating the results obtained in the first experiment. During the HR experiment, the RR was also estimated by both, our system and the oximeter. The purpose was to analyze spontaneous

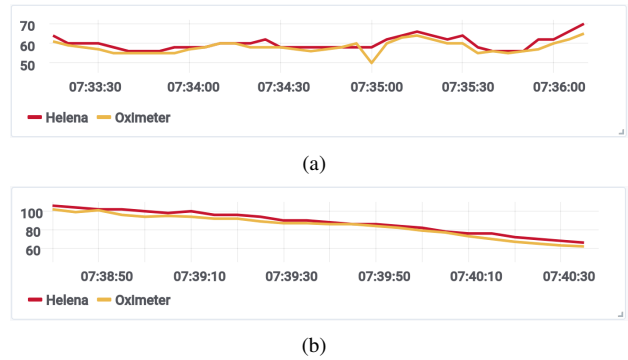


Fig. 10: HR visual comparison between Helena and an oximeter. (a) Before exercising. (b) After exercising.

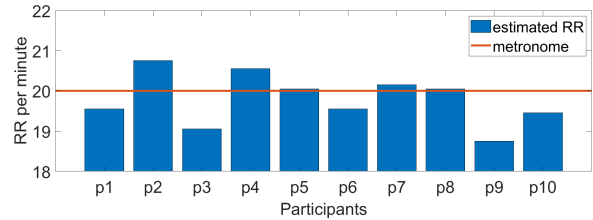


Fig. 11: RR results from controlled respiration using a metronome using a frequency of 20 breath per minute.

breathing. We obtained 36 and 24 measurements estimations during resting and active mode respectively from each person. The results from the two modes are shown in Fig. 12, having a mean error of 1.56 rpm during the resting mode and 0.61 rpm during the active mode. It is noteworthy that the error in the active mode is smaller because the deep breathing generates a marked difference between the inhalation and exhalation phases improving the envelope calculation.

4) **Movements:** The objective of the experiment is the body movement detection. However, the experiment was designed to collect data that will be used to develop future features such as the movement location. During it, we asked the participants to move different parts of their body one at a time every 5 seconds. The body part used were the left hand, right hand, left leg, right leg, head, and shoulders. We told the participant which part he/she needed to move according to a pre-established pattern. A total of 240 events were used for calculating false negatives and accuracy. The movements were classified into

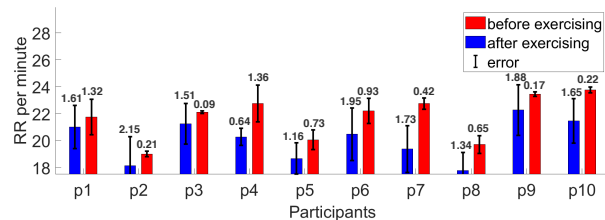


Fig. 12: Results and errors from spontaneous RR calculated by Helena.

TABLE III: Matrix confusion for posture change detection.

To	Recognized as		Eval
	Change	No Change	
Back	110	10	91.67
Chest	115	5	95.83
Right	108	12	90.00
Left	105	15	87.50
Avg.			91.25

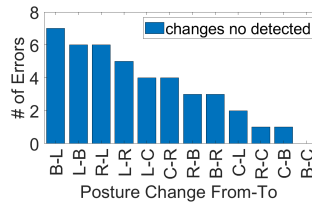


Fig. 13: Posture change transition error. B(Back),L(Left), R(Right),C(Chest)

two groups, “upper movements” (head, arms, and hands) and “lower movements” (legs and feet). The system did not detect 5 movements from the 240 generated, obtaining an accuracy of 97.92%. All of these 5 movements were from lower movements specifically from the feet located outside the bed generating lower magnitude lower than any on-bed event.

5) *Posture Changes*: We organized a pattern where the participant had to change to one position from the other three positions. For example, starting from “left”, move to “back”, then “chest”, “back”, “right”, “back”, and so on. We collected 48 posture changes from each participant. The results obtained after the evaluation are presented in Table III. A total of 438 posture changes were successfully recognized getting an accuracy of 91.25%. Fig. 13 shows the posture change failures from one position to another. As signals from the “back” and “left” have similar characteristics, the posture changes with the highest error were from “back” to the “left” and vice versa. On the other hand, “chest” and “back” posture signals are very different, which leads in fewer errors from “back” to “chest” and vice versa with just one failure.

B. Outside experiment:

We set up the experiment in 13 different homes with varied environments, beds, and background noise. We got the help from 25 participants. Specifications of the different mattress,

size, materials, and distance between floor and boxes(frames) of the 25 beds are listed in Table IV. The experiment was established for 5 continuous days. Due to some limitation with the number of units and the FDA devices used to validate our results, we experimented during 4 different weeks.

1) *On-bed, Off-bed and sitting experiment*: We established windows for analyzing on and off-bed. The off-bed window was set between 9 am and 5 pm. Participants confirmed it was their time to be out of their homes. For the on-bed hours, a window was established between 9 pm and 6 am. A limitation of this experiment is that we could not perform sitting validations. However, we analyzed the raw data and the HR and RR results. We did not find any HR and RR calculation outside those expected. We took as expected values for HR between 40 and 140 and respiration between 12 and 25. Also, we considered expected continuous variations between estimations not greater than 8 bpm for HR and 6 for rpm for RR. For example, the HR values of a false on-bed can vary from 62 to 78 bpm in 5 seconds and for RR from 18 to 26 rpm. We did not find unexpected values during the 125 nights. We confirmed that no HR or RR was estimated while the participants were sitting on the bed. Table IV shows in two columns the false positives detected per house during the test. The false on-bed column reflects the false positives on-bed or the times when the system detected a person on-bed during off-bed hours. During the entire experiment, five false on-bed detection were presented in two different houses. In house number 6, four false on-bed were detected with a duration smaller than 5 minutes. We analyzed the signal and realized that the environment was very noisy due to the house construction. Three false on-bed detection occurred in the bed next to the laundry room. During this time we found two mixed signals that correlated as well as HR signal. In another hand, the false on-bed detection on house number 12 was analyzed, and a cardiac signal was found with an HR average of 120 bpm. We found it was from the participant’s dog who usually sleeps at the bottom of the bed.

TABLE IV: Outside test details and results. Relevant information from the participants, environments, and beds is shown. The results obtained in each of the parts of the system are presented. The highlights are summarized in the last row.

#	House	Gender	Age	Weight	Location	Room Location	Floor Type Under Carpet	Bed Frame	Mattress Material	Mattress Height	Ave-HR \pm Error	RR	False On-bed	False Off-bed	Posture Change Acc	Fall Acc
1	1	Male	39	196	Bogart	2 Floor	Wood	No	Innerspring	14.5	66bpm \pm 1.32	21.3rpm	0	0	92.86	100
2		Female	37	154	Bogart	2 Floor	Wood	No	Memory foam	11.5	72bpm \pm 1.59	22.2rpm	0	0	90.54	100
3	2	Male	21	121	Bogart	2 Floor	Wood	No	Memory foam	8	64bpm \pm 2.08	22.2rpm	0	1	-	100
4		Male	23	147	Bogart	2 Floor	Wood	No	Memory foam	8	58bpm \pm 2.13	18.1rpm	0	0	-	100
5	6	Female	62	114	Bogart	1 Floor	Concrete	No	Innerspring	10	54bpm \pm 1.27	20.6rpm	0	0	94.44	75
6		Male	19	136	Bogart	1 Floor	Concrete	No	Memory foam	8	76bpm \pm 2.68	16.4rpm	0	0	-	100
7	3	Male	33	172	Athens	4 Floor	Wood	Yes	Hybrid	11	58bpm \pm 1.97	20.1rpm	0	0	87.30	100
8		Female	24	127	Athens	2 Floor	Concrete	Yes	Innerspring	9	63bpm \pm 1.57	19.3rpm	0	0	-	100
9	5	Male	22	143	Athens	2 Floor	Wood	Yes	Innerspring	9	67bpm \pm 2.73	19.5rpm	0	0	-	100
10		Male	19	204	Alpharetta	2 Floor	Wood	Yes	Hybrid	11	78bpm \pm 1.68	20.0rpm	3	0	-	100
11	6	Male	24	167	Alpharetta	2 Floor	Wood	Yes	Hybrid	11	54bpm \pm 1.58	16.7rpm	1	0	-	100
12		Male	51	154	Alpharetta	2 Floor	Wood	Yes	Hybrid	11	77bpm \pm 5.28	20.9rpm	0	0	94.34	100
13	7	Male	49	200	Alpharetta	2 Floor	Wood	Yes	Memory foam	10	83bpm \pm 1.91	16.2rpm	0	0	-	100
14		Male	24	183	Alpharetta	1 Floor	Concrete	Yes	Memory foam	10	63bpm \pm 1.61	17.4rpm	0	0	92.31	100
15	8	Female	64	128	Alpharetta	1 Floor	Concrete	Yes	Memory foam	10	55bpm \pm 1.29	19.3rpm	0	0	93.33	100
16		Male	41	205	Watkinsville	1 Floor	Wood	No	Memory foam	10	69bpm \pm 1.95	20.1rpm	0	0	-	100
17	9	Male	25	161	Roswell	3 Floor	Wood	Yes	Hybrid	14.5	81bpm \pm 5.18	19.7rpm	0	2	-	75
18		Female	27	144	Roswell	3 Floor	Wood	Yes	Hybrid	14.5	74bpm \pm 6.30	19.1rpm	0	0	-	100
19	10	Male	33	231	Sandy Springs	2 Floor	Wood	Yes	Memory foam	7	81bpm \pm 1.83	20.4rpm	0	0	-	100
20		Female	18	143	Sandy Springs	2 Floor	Wood	Yes	Memory foam	7	72bpm \pm 2.18	21.2rpm	0	0	91.49	100
21	11	Female	59	169	Sandy Springs	2 Floor	Wood	No	Memory foam	7	63bpm \pm 1.59	21.1rpm	0	0	-	100
22		Male	34	139	Northcross	2 Floor	Wood	Yes	Hybrid	11.5	64bpm \pm 3.80	16.2rpm	0	0	-	75
23	12	Male	32	141	Dunwoody	9 Floor	Concrete	Yes	Hybrid	11.5	78bpm \pm 3.24	22.0rpm	1	0	-	100
24		Female	44	196	Marietta	2 Floor	Wood	Yes	Innerspring	9.5	75bpm \pm 1.63	18.8rpm	0	0	-	100
25	13	Female	58	146	Marietta	2 Floor	Wood	Yes	Innerspring	9.5	61bpm \pm 1.77	16.7rpm	0	0	-	100
Summary		Males 16 Females 9	Min 18 Max 64	Min 112 Max 231	Cities 9	Levels 5	Types 2	Yes 17 No 8	Innerspring 6 Memory 11 Hybrid 8	Min 7 Max 14.5	HR Avg. 68.24 Error Avg. 2.41	Min 16.2 Max 22.2	Total 5	Total 4	Avg. 92.08	Avg. 97

The system was able to detect and calculate the dog’s HR. The accuracy calculated per day and hour would be 96% and 99.5% respectively. The false off-bed column shows the false exits from the bed. It happens when the system cannot detect the heartbeat due to poor posture and/or a thick object used between the body and the mattress. The accuracy calculated per day and per hour was 97.6% and 99.73%. The solution proposed for both false detection is to recognize a big event before “bed status” change. These events are induced when the person sitting, lying down, leaving the bed or changing positions. With this approach, the eight detection in total can be reduced to one.

2) **Heart and respiration rate experiment:** We used an FDA class 2 medical device, Apple Watch Series 4 [35], to validate the accuracy of our HR method. The Apple Watch provides HR continuous reading in a range between 3 to 10 seconds. One of the limitations is the battery life since it only allows collecting around 5 hours of continuous HR. Participants used an AppleWatch for 5 days at bedtime. We selected it because it is one of the most accurate devices on the market calculating HR with an average error of 2.99 bpm [36]. AppleWatch incorporates some errors during the HR estimation where the changes between 2 consecutive readings are larger than 25 bpm, and it is not normal even is the person is having a panic attack [37]. Fig. 14 shows the graphic results between AppleWatch and our system in different tests. In both figures, our method follows the pattern established by the AppleWatch. Also, the errors from the AppleWatch can be observed. The largest different during the test is shown at 2:40 am in Fig. 14a. We checked other indicators at the same time, and we observed that in these 12 minutes, several movements were detected. We can infer that the person was awake at this time. In the same figure, at 3:20 am, there are 10 minutes of missing results by our system because it detected off-bed status. It was confirmed by the participant.

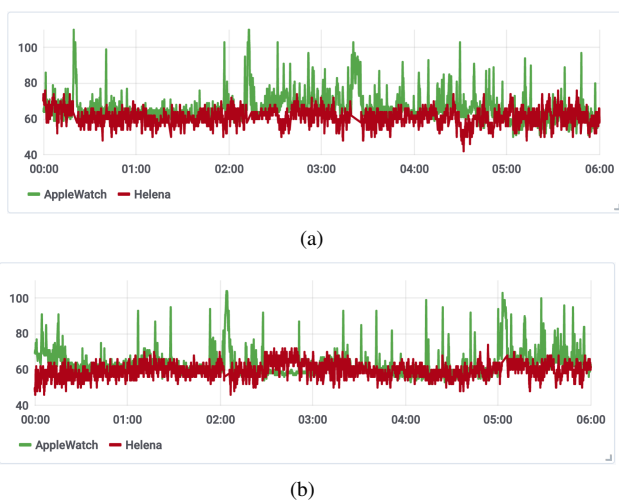


Fig. 14: HR comparison between Apple Watch Version 4 and Helena. (a) Participant 17. (b) Participant 20.

Table V summarizes the results of the entire HR exper-

iment, showing the mean absolute error (MAE) and the peaks introduced by the AppleWatch. Note that the error decreases according to the growth of the time window, and the AppleWatch added more than three errors in one hour. We set 15 minutes windows for comparison due to many commercial devices calculate HR at this frequency. The MAE of the system is 2.41 bpm even when the AppleWatch incorporates during that time an unreliable peak of data. Devices on the market calculate HR with an average error between 2 and 5 bpm. The error obtained in our experiment shows that our system is within the confidence range estimating HR. Table VI shows a ranking summary of the MAE using 15 minutes window. The four best results showed an average error of less than 1.6 bpm. According to Table IV, the common variable to obtain these results is the type of mattress, in this case innerspring. The same variable affects the system performance because in the highest four errors detected, the type of mattresses was a hybrid. The hybrid bed has two layers innerspring on the bottom and foam on the top. After checking the signal, we noted that the bed material affects the energy signal. However, there are some exceptions as participants 7, 10 and 11. It is because two other variables influence the energy signal such as person weight and mattress height. In those cases, the participants obtained a lower error than the average due to their weight and heartbeat strength. Even when participant 18 is an overweight person, the error obtained in this experiment was the highest because the participant’s bed is thicker.

TABLE V: HR mean absolute error from Helena and abnormal peaks during estimations.

Average Time	Mean Absolute Error \pm STD	Abnormal Peaks from	
		AppleWatch	Helena
1 minute	4.28 \pm 2.80 bpm	0.059	0
3 minutes	4.01 \pm 2.53 bpm	0.183	0
5 minutes	3.43 \pm 2.23 bpm	0.302	0
10 minutes	2.89 \pm 2.06 bpm	0.611	0
15 minutes	2.41 \pm 1.88 bpm	0.926	0
30 minutes	1.76 \pm 1.56 bpm	1.866	0
1 hour	1.41 \pm 0.70 bpm	3.384	0

TABLE VI: Mean absolute error rank of HR validation.

Rank	Participant	Mean Absolute Error \pm STD	Abnormal Peaks from	
			AppleWatch	Helena
1	C5	1.27 \pm 1.29	0.544	0
2	C15	1.29 \pm 1.82	0.742	0
3	C1	1.32 \pm 1.59	1.032	0
4	C8	1.57 \pm 1.26	0.786	0
22	C22	3.80 \pm 3.40	1.143	0
23	C17	5.18 \pm 3.47	0.887	0
24	C12	5.28 \pm 3.90	0.786	0
25	C18	6.30 \pm 4.73	1.446	0

Validating the respiration rate (RR) was more difficult. Affordable on-the-market devices for monitoring RR have low accuracy and are difficult to wear overnight. For this reason, we only were able to evaluate the results based on the “range of confidence” and the “acceptable variability”. The “range of confidence” was established between 13 and 25 rpm as we worked only with healthy participants. The

“acceptable variability” means no abrupt changes between one RR estimation and another in a shorter time. None of the participants were outside of the “range of confidence”, and the highest variability was obtained by participant 18, with 4 rpm different between two consecutive measurements. Table IV shows the RR average from each participant.

3) **Posture Change and Movement experiment:** We obtained permission from 8 participants to install infrared cameras with motion detection [38]. Fig. 15 shows the camera used and images from the video recorded. The cameras were configured to record video during the bedtime between 9 pm to 6 am. Additionally, cam alerts were activated to record 12 seconds of video after movement detection. The alerts helped us to validate true positives, false positives and true negatives. In each alert, we verified if there was a posture change or not contrasting it with the results of our system. Additionally, we verified the continuous video recorded in cases where our system registered a posture change, but the alert was not emitted by the camera. This specific case occurred when the person made two continuous posture change and the alert was activated just the first time.



Fig. 15: Posture change validation. Camera used in the validation and images taken during the experiment. (a) The infrared camera with motion detection. (b) Lady sleeping on the right. (c) Second lady sleeping on the back. (d) Man sleeping on the left.

The test results are shown in Table VII. We noted that the failures produced by the system occurred in 76.31% of cases when the posture change was from left to back or vice versa, similar to results registered in the laboratory test. The average accuracy for the spontaneous posture change is 92.08% which validates results obtained in the simulated posture change test performed in the laboratory. We were unable to perform a quantitative evaluation of movements during the bedtime windows because slight movements detected by the system are not detected by the camera. However, our system detected movements in all alerts not classified as a posture change.

4) **Fall-down:** Because falls from bed are not common events to be validated in a real environment, we performed simulated falls when we installed the sensors in different environments. Two falls on each bedside were simulated on each bed. Only 3 events were not classified as a fall from bed having an accuracy of 97%. Throughout the experiment, we did not detect any false fall from the bed. Even when the method was trained with different fall positions, people, environments, and beds, the data were simulated falls. For this reason, we cannot guarantee the same level of accuracy in spontaneous

TABLE VII: Posture change validation results.

Parti	Event detected by the camera	Real posture changes	Changes detected		Acc
			yes	no	
C1	60	56	52	4	92.86
C2	76	74	67	7	90.54
C5	54	54	51	3	94.44
C7	69	63	55	8	87.30
C12	57	53	50	3	94.34
C14	66	65	60	5	92.31
C15	62	60	56	4	93.33
C22	51	47	43	4	91.49
Avg.					92.08

falls. However, we plan to integrate another sensor installed on the floor to combine the events that occur in the bed and on the floor, to provide a higher level of confidence [6].

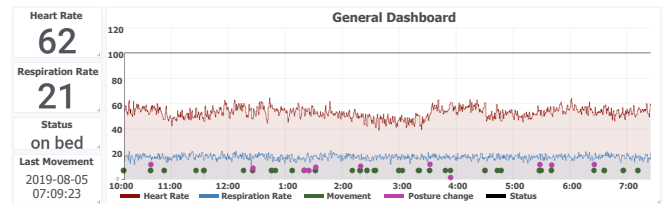


Fig. 16: System results dashboard from one participant at Magnolia Senior Care Facility.

C. Senior Care Center Test

Because two previous tests are performed with healthy people and under 60 years, we decided to perform an additional test with senior people. Two units were installed for two days in Magnolia Senior Care facility located in the city of Loganville GA. We received the approval by the manager, the participants, and their families. The participants were 87 years old and 147 pounds gentleman, and a 74 years old and 132 pounds lady. The on-bed, off-bed and sitting status, were confirmed by the nurses. The HB and RR were monitored in real-time from our central dashboard. The values of both HR and RR were normal throughout the process. No false fall from bed was detected. We could not perform posture change or movement validations. Fig. 16 shows the monitoring dashboard during part of the process, which allows seeing the report in real-time showing the last 5 minutes results and also to check historical results.

VII. CONCLUSION

An accurate and suitable pervasive sleep monitoring system (Helena) based on a contact-free bed-mounter sensor is proposed in this paper. Novel methods for heart rate and respiration rate estimations have been introduced only based on heart vibrations on the bed. For the first time, a non-intrusive method to detect and alert falls from bed has been introduced with an accuracy higher than 95%. The system also allows real-time monitoring of movements and posture changes. The performance has been multiple times tested on different people, beds, environments to determine its accuracy and has been compared with FDA approved wearable devices reaching promising results.

REFERENCES

- [1] The World Bank Data, "World Bank's total population and age/sex distributions of the United Nations Population," 2017. [Online]. Available: <https://data.worldbank.org/indicator/SP.POP.65UP.TO>
- [2] A. Roberts, S. Ogunwole, L. Blakeslee, and M. Rabe, "The population 65 years and older in the united states," no. ACS-38, 2016.
- [3] F. Li, J. Clemente, M. Valero, Z. Tse, S. Li, and W.-Z. Song, "Smart home monitoring system via footstep induced vibrations," *IEEE Systems Journal*, 2019, Online.
- [4] J. Clemente, W. Song, M. Valero, F. Li, and X. Li, "Indoor person identification and fall detection through non-intrusive floor seismic sensing," in *5th IEEE International Conference on Smart Computing (SMARTCOMP)*, 2019, pp. 417–424.
- [5] S. Pan, T. Yu, M. Mirshekari, J. Fagert, A. Bonde, O. J. Mengshoel, H. Y. Noh, and P. Zhang, "FootprintID: Indoor Pedestrian Identification through Ambient Structural Vibration Sensing," *Proceedings of the ACM on Interactive, Mobile, Wearable and Ubiquitous Technologies*, vol. 1, no. 3, p. 89, 2017.
- [6] J. Clemente, F. Li, M. Valero, and W. Song, "Smart seismic sensing for indoor fall detection, location and notification," *IEEE Journal of Biomedical and Health Informatics*, 2019, Online.
- [7] R. N. Aurora, S. P. Patil, and N. M. Punjabi, "Portable Sleep Monitoring for Diagnosing Sleep Apnea in Hospitalized Patients With Heart Failure," *Chest*, 2018.
- [8] F. Li, J. Clemente, and W. Song, "Non-intrusive and non-contact sleep monitoring with seismometer," in *2018 IEEE Global Conference on Signal and Information Processing (GlobalSIP)*. IEEE, 2018, pp. 449–453.
- [9] P. Kowallik and W. Hubert, "Method and device for sleep monitoring," Jun. 2004, uS Patent 6,752,766.
- [10] K.-L. Hsiao, "What drives smartwatch adoption intention? comparing apple and non-apple watches," *Library Hi Tech*, vol. 35, no. 1, pp. 186–206, 2017.
- [11] L. Jeon and J. Finkelstein, "Consumer sleep tracking devices: a critical review," *Digital Healthcare Empowering Europeans: Proceedings of MIE2015*, vol. 210, p. 458, 2015.
- [12] E. Jovanov, "Preliminary analysis of the use of smartwatches for longitudinal health monitoring," in *2015 37th Annual International Conference of the IEEE Engineering in Medicine and Biology Society (EMBC)*. IEEE, 2015, pp. 865–868.
- [13] K. M. Diaz, D. J. Krupka, M. J. Chang, J. Peacock, Y. Ma, J. Goldsmith, J. E. Schwartz, and K. W. Davidson, "Fitbit®: An accurate and reliable device for wireless physical activity tracking," *International journal of cardiology*, vol. 185, pp. 138–140, 2015.
- [14] L. Leppäkorpi, "Beddit is a new kind of device and app for tracking & improving sleep and wellness," *Beddit Is a New Kind of Device and App for Tracking & Improving Sleep and Wellness*, 2014.
- [15] "Nokia Withings Sleep Pad," <https://www.withings.com/us/en/sleep>, last Accessed: 2019-04-30.
- [16] M. Helfand, V. Christensen, and J. Anderson, "Technology assessment: early sense for monitoring vital signs in hospitalized patients," 2016.
- [17] W.-Z. Song, R. Huang, M. Xu, B. A. Shirazi, and R. LaHusen, "Design and Deployment of Sensor Network for Real-Time High-Fidelity Volcano Monitoring," *IEEE Transaction on Parallel and Distributed Systems*, vol. 21, no. 11, pp. 1658–1674, 2010. [Online]. Available: <http://dx.doi.org/10.1109/TPDS.2010.37>
- [18] W. Song, L. Shi, G. Kamath, Y. Xie, and Z. Peng, "Real-time In-situ Seismic Imaging: Overview and Case Study," in *SEG Annual Meeting 2015*, Society of Exploration Geophysicists. Society of Exploration Geophysicists, 2015. [Online]. Available: <http://dx.doi.org/10.1190/segam2015-5833447.1>
- [19] F. Li and W. Song, "Automatic arrival identification system for real-time microseismic event location," in *SEG Technical Program Expanded Abstracts 2017*, S. E. of Geophysicists, Ed., 2017, pp. 2934–2939. [Online]. Available: <http://dx.doi.org/10.1190/segam2017-17667176.1>
- [20] J. Clemente, F. Li, M. Valero, A. Chen, and W. Song, "Asis: Autonomous seismic imaging system with in-situ data analytics and renewable energy," *IEEE Systems Journal*, 2019, Online.
- [21] S. Pan, N. Wang, Y. Qian, I. Velibeyoglu, H. Y. Noh, and P. Zhang, "Indoor person identification through footstep induced structural vibration," in *Proceedings of the 16th International Workshop on Mobile Computing Systems and Applications*. ACM, 2015, pp. 81–86.
- [22] Z. Jia, M. Alaziz, X. Chi, R. E. Howard, Y. Zhang, P. Zhang, W. Trappe, A. Sivasubramaniam, and N. An, "HB-phone: a bed-mounted geophone-based heartbeat monitoring system," in *Information Processing in Sensor Networks (IPSN), 2016 15th ACM/IEEE International Conference on*. IEEE, 2016, pp. 1–12.
- [23] M. Alaziz, Z. Jia, J. Liu, R. Howard, Y. Chen, and Y. Zhang, "Motion scale: A body motion monitoring system using bed-mounted wireless load cells," in *Connected Health: Applications, Systems and Engineering Technologies (CHASE), 2016 IEEE First International Conference on*. IEEE, 2016, pp. 183–192.
- [24] Z. Jia, A. Bonde, S. Li, C. Xu, J. Wang, Y. Zhang, R. E. Howard, and P. Zhang, "Monitoring a Person's Heart Rate and Respiratory Rate on a Shared Bed Using Geophones," 2017.
- [25] C. E. Krohn, "Geophone ground coupling," *Geophysics*, vol. 49, no. 6, pp. 722–731, 1984.
- [26] "GeoPhone." [Online]. Available: <https://www.sparkfun.com/products/11744>
- [27] E. Upton, "Raspberry Pi 3," *URL* <https://www.raspberrypi.org/products/raspberry-pi-3-model-b>, 2016.
- [28] Influxdata Inc, "InfluxDB," 2019. [Online]. Available: <https://www.influxdata.com/>
- [29] Grafana Labs, "Grafana," 2018. [Online]. Available: <https://grafana.com/>
- [30] R. S. Holambe and M. S. Deshpande, "Nonlinear measurement and modeling using teager energy operator," in *Advances in Non-Linear Modeling for Speech Processing*. Springer, 2012, pp. 45–59.
- [31] C. Cortes and V. Vapnik, "Support-vector networks," *Machine learning*, vol. 20, no. 3, pp. 273–297, 1995.
- [32] L. Wang, K. Huang, K. Sun, W. Wang, C. Tian, L. Xie, and Q. Gu, "Unlock with Your Heart: Heartbeat-based Authentication on Commercial Mobile Phones," *Proceedings of the ACM on Interactive, Mobile, Wearable and Ubiquitous Technologies*, vol. 2, no. 3, p. 140, 2018.
- [33] A. Johansson, "Neural network for photoplethysmographic respiratory rate monitoring," *Medical and Biological Engineering and Computing*, vol. 41, no. 3, pp. 242–248, 2003.
- [34] R. Ravichandran, E. Saba, K.-Y. Chen, M. Goel, S. Gupta, and S. N. Patel, "Wibreathe: Estimating respiration rate using wireless signals in natural settings in the home," in *2015 IEEE International Conference on Pervasive Computing and Communications (PerCom)*. IEEE, 2015, pp. 131–139.
- [35] "AppleWatch4." [Online]. Available: <https://www.apple.com/apple-watch-series-4/>
- [36] E. A. Thomson, K. Nuss, A. Comstock, S. Reinwald, S. Blake, R. E. Pimentel, B. L. Tracy, and K. Li, "Heart rate measures from the apple watch, fitbit charge hr 2, and electrocardiogram across different exercise intensities," *Journal of sports sciences*, vol. 37, no. 12, pp. 1411–1419, 2019.
- [37] K. Spiegelhalter, M. Hornyak, S. D. Kyle, D. Paul, J. Blechert, E. Seifritz, J. Hennig, L. Tebartz van Elst, D. Riemann, and B. Feige, "Cerebral correlates of heart rate variations during a spontaneous panic attack in the fmri scanner," *Neurocase*, vol. 15, no. 6, pp. 527–534, 2009.
- [38] "Wyze2." [Online]. Available: <https://www.wyze.com/product/wyze-cam-v2/>